1998ASPC..155..182K

2^{nd} *Advances in Solar Physics Euroconference*
Three-Dimensional Structure of Solar Active Regions
ASP Conference Series, Vol. 155, 1998
C. E. Alissandrakis, and B. Schmieder, eds.

Suprathermal Electrons in Non-flaring Active Regions

Karl-Ludwig Klein

Observatoire de Paris, DASOP & CNRS URA 2080, F-92195 Meudon

Abstract. Non-maxwellian electron populations generate bright emissions at decimetric and longer wavelengths, even in the absence of conspicuous energy deposition identified as a flare. The paper discusses three topics: (i) electron beam production in the low corona associated with jets of cool and hot material, (ii) "high coronal" acceleration ($\geq 0.5\ R_\odot$ above the photosphere), (iii) long-lasting electron acceleration (up to several days) in noise storms. These phenomena can now be situated with respect to coronal plasma structures visualised through imaging in microwaves (cm-λ), visible light, EUV and X-rays. The acceleration occurs on similar timescales as in flares, but mostly at heights where emission during flares is outshone by the lower corona. These regions are a possible site for the acceleration of particles injected into interplanetary space, and their study will allow us to put constraints on the relationship between the evolution of large-scale coronal structures and small-scale processes of energy release.

1. Introduction

Energy release processes in the solar corona are measured over many decades, from the smallest detectable "microflares" ($\sim 10^{25}$ ergs; Shimizu 1995) to a few "giant" events involving possibly $\sim 10^{34}$ ergs (Kane et al. 1995). There seems to be no basic difference between large flares and microflares, since parameters related to the released energy display a continuous distribution (Hudson 1991, Crosby et al. 1993, Shimizu 1995, Vilmer & Trottet 1997). While energetic events generate emission throughout the electromagnetic spectrum, low-energy non-maxwellian electron populations in the corona are revealed chiefly by radio emission at decimetric and longer wavelengths. They allow us to investigate to which extent processes of explosive energy release that probably involve magnetic reconnection are at work in non-flaring active regions. The radio signatures, identified through properties such as high brightness, strong circular polarization or remarkable spectral structure, are emitted at heights greater than several 10^4 km above the photosphere. We loosely refer to the height range up to 1 $R_\odot$ as the middle corona, and to greater altitudes as the high corona.

This review presents observations of suprathermal electron populations in the corona related with active regions and discusses observational constraints on the sites and circumstances of their production in the absence of flares. This means nothing more than a restriction to events with comparatively low energy budget or without energy input in the low atmosphere, so that there will be no

© Astronomical Society of the Pacific • Provided by the NASA Astrophysics Data System

1998ASPC..155..182K

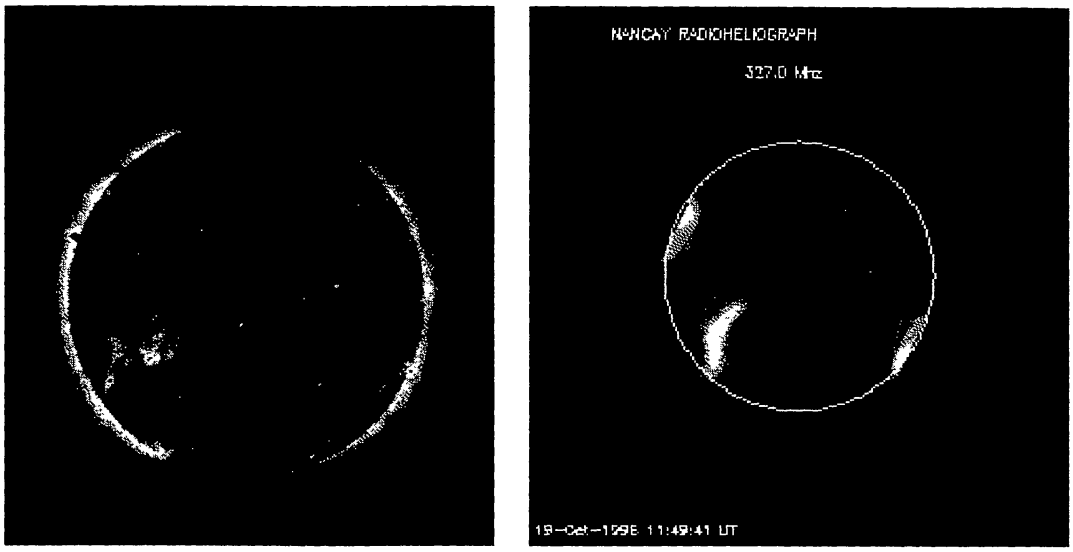

Figure 1. X-ray (*SoHO/EIT*, 195 Å line, temperature $1.6 \cdot 10^6$ K; courtesy EIT consortium, J.P. Delaboudinière) and radio image (*Nançay Radioheliograph*, 327 MHz/91 cm) of the quiet corona.

Hα or hard X-ray signature. Emphasis is laid on joint radio diagnostics and imaging observations of coronal plasma structures.

The outline of the paper is as follows: Section 2. illustrates decimetric and metric radio emission from the corona. The best known nonthermal electron distributions in the corona are beams. A short introduction to the mechanism by which they generate radio waves is given in Section 3. Observations of beam production associated with jets of material in the low corona are summarized and mechanisms which might relate the two phenomena are outlined. Acceleration in the middle and high corona, which is possibly related with electrons detected in interplanetary space, is then discussed. Trapped electron distributions above active regions that imply the time-extended acceleration over up to several days and are therefore a key example of quasi-steady nonthermal energy release are presented in Section 4.

Recent reviews related to the same subject are Benz (1994, 1997), Klein (1994) and Vilmer & Trottet (1997). Particle acceleration processes during flares, which are relevant to the present subject, too, were reviewed by Miller et al. (1997).

2. The Solar Corona at Radio Wavelengths

The coronal plasma emits broadband radio emission from centimetric to decametric waves through thermal bremsstrahlung (Sheridan & McLean 1985). Its brightness is roughly a measure of the square of the electron density integrated along the ray trajectory. The diffuse emission in decimetric and metric waves (Figure 1) comes mainly from arches above the line of photospheric magnetic field inversion (e.g. Lantos & Alissandrakis 1996). The density depletion in a coronal hole is clearly seen (cf. Lantos et al. 1987, and references therein).

© Astronomical Society of the Pacific • Provided by the NASA Astrophysics Data System

1998ASPC..155..182K

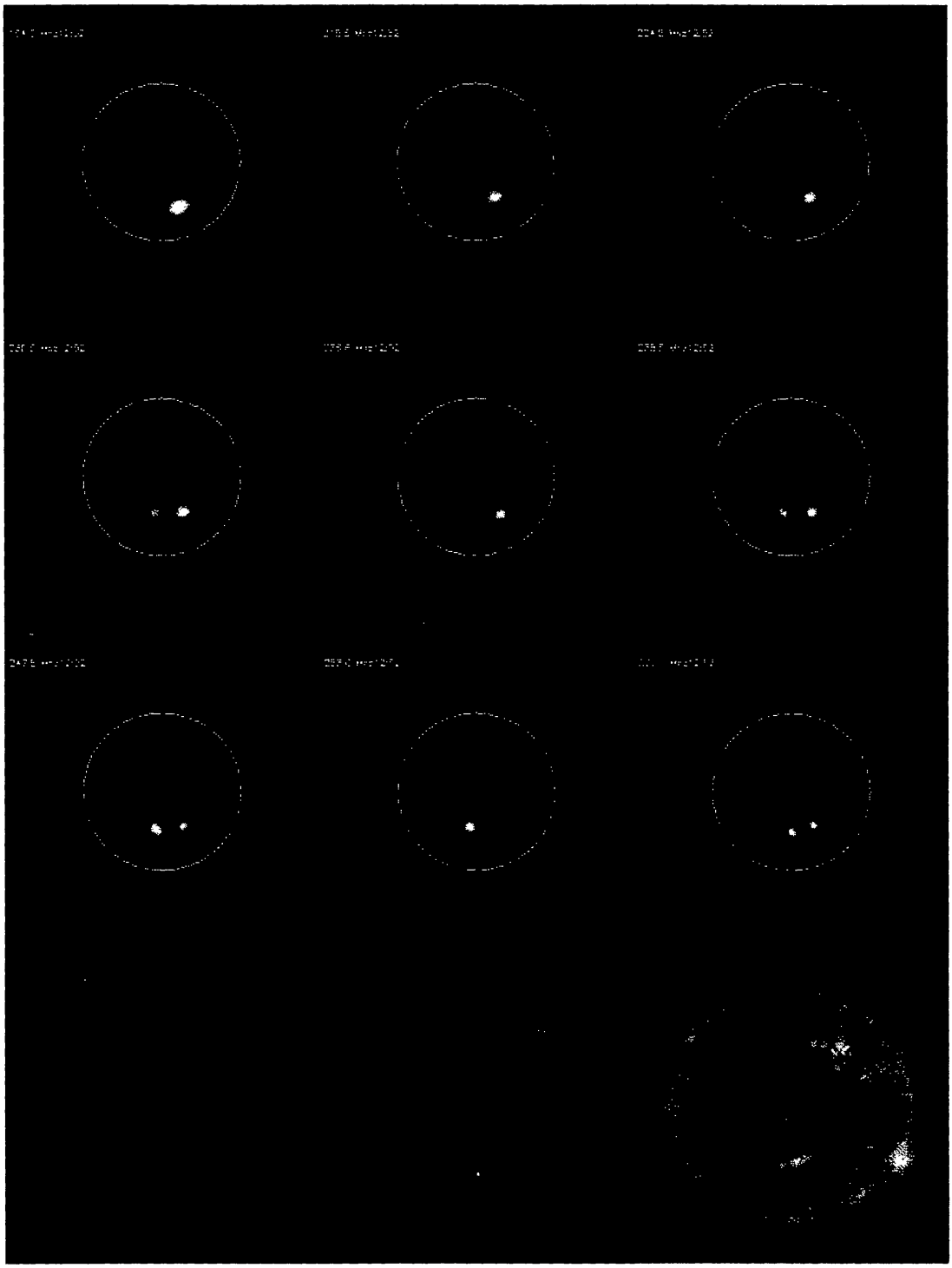

Figure 2. A noise storm at ten decimetric and metric radio wavelengths (frequency increasing from left to right and top to bottom, *Nançay Radioheliograph*). The sources lie above active region structures outlined by the *SoHO/EIT* image at 195 Å (bottom right). Comparison with the *SoHO/MDI* magnetogram (bottom line, centre) shows that the high-frequency radio sources lie on either side of the photospheric line of magnetic field reversal, while the low-frequency source lies above this line.

© Astronomical Society of the Pacific • Provided by the NASA Astrophysics Data System

1998ASPC..155..182K

In the presence of an active region the radio corona often looks quite different (Figure 2): the radioheliograms at ten frequencies show localized bright sources that outshine the background corona. This radio emission (called a noise storm) may last several hours or even days and reveals the acceleration of electrons to suprathermal, but subrelativistic energies (~10 keV; cf. Section 4) over such durations. The spatial distribution of the emission suggests that the electrons radiate in large-scale loop systems connected with the active region, where low-frequency emission comes from the vicinity of the summits of the higher loops, while the high-frequency emission is generated near the footpoints. The frequency dispersion of the radio sources translates the variation of the thermal electron density in the coronal structures, since the radiation is emitted close to the electron plasma frequency, so that high frequencies correspond to high electron densities. This is a general feature of decimetric and metric emission from the active corona that will be discussed further in the next section.

3. Electron Beams

3.1. Plasma Emission from Electron Beams

The clearest spectral signature of non-maxwellian electrons in the corona is due to beams which induce charge oscillations in the plasma through which they propagate. The charge oscillations (Langmuir waves) occur in the vicinity of the local electron plasma frequency,

$$\nu_{pe} = \sqrt{\frac{n_e}{5 \cdot 10^8 \text{ cm}^{-3}}} \cdot 200 \text{ MHz} \tag{1}$$

where n_e is the thermal electron density. The Langmuir waves remain trapped in the source, but can be scattered into electromagnetic waves by the polarization cloud of thermal ions or through the coupling with other plasma waves, either ion sound waves (frequency $\nu_s \ll \nu_{pe}$) or other Langmuir waves. An alternative to the first mechanism is the decay of a Langmuir wave into an electromagnetic wave and an ion-sound wave. While the scattering off the polarization cloud of the ions does not alter the frequency, wave-wave interactions give rise to an electromagnetic wave whose frequency is the sum of those of the parent waves:

$$\begin{aligned} \nu = \nu_{pe} \pm \nu_s \simeq \nu_{pe} \\ \nu = 2\nu_{pe} \end{aligned} \tag{2}$$

These relations can be understood as analogues of energy conservation in a quasi-quantum mechanical formalism (cf. e.g. Melrose 1980, Benz 1993). The resulting radio waves hence occur near the fundamental or harmonic of the local plasma frequency, in certain cases at both.

In the middle corona the electromagnetic wave production lasts for a short time only (~1 s), so that the observed signature is a pulse at a given frequency, which shifts to different frequencies as the exciter propagates into regions of different thermal electron densities. The emission most frequently seen comes

© Astronomical Society of the Pacific • Provided by the NASA Astrophysics Data System

1998ASPC..155..182K

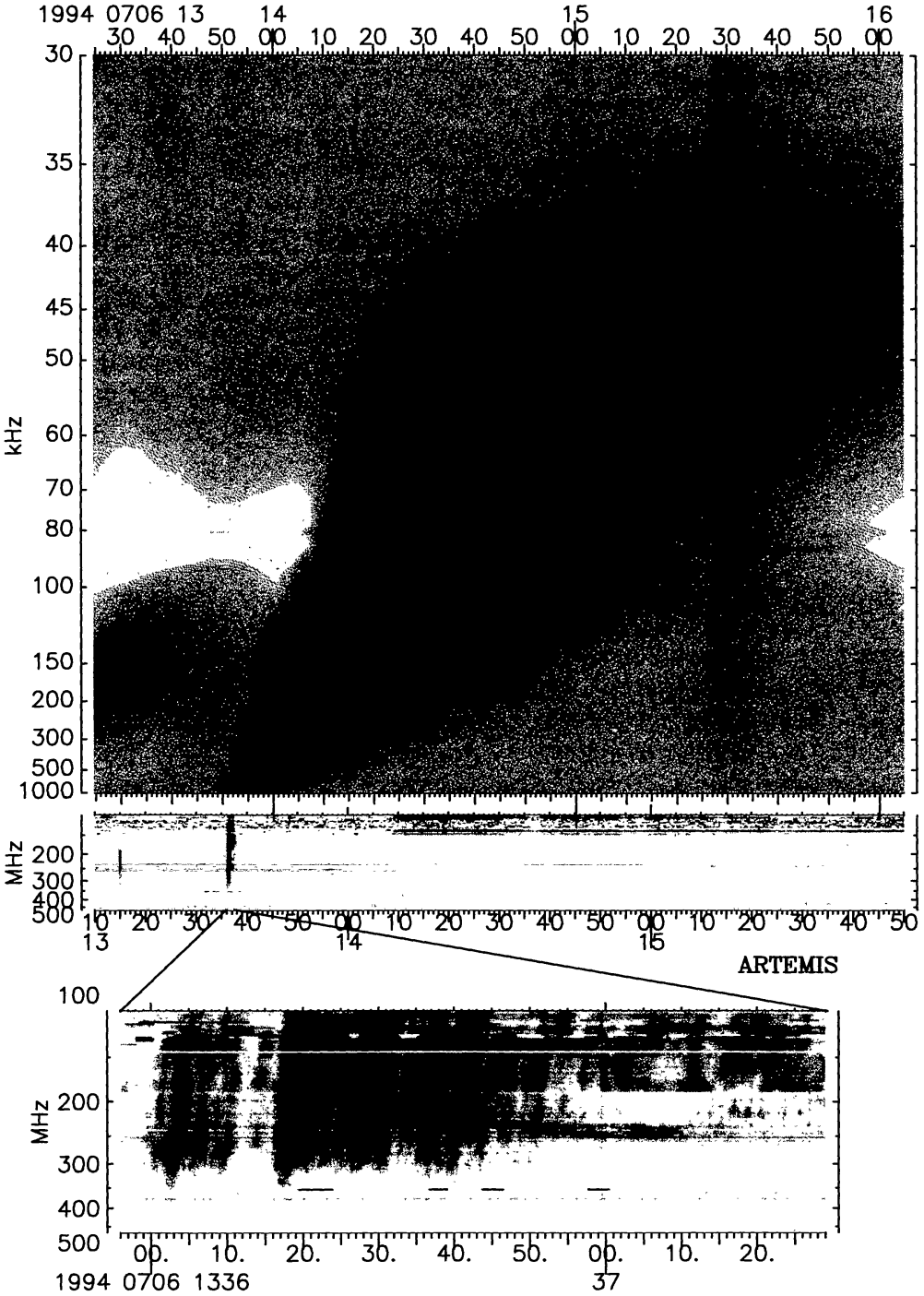

Figure 3. A group of type III bursts observed over a wide frequency range, emitted by electron beams that propagate from the low corona (500 MHz; *Artemis* spectrograph, Space Res. Dept. of Paris Observatory) to 1 UA (30 kHz, *Ulysses/URAP*). Numerous bursts at high frequencies merge into an apparently simple burst below 1 MHz, demonstrating that individual type III bursts may be composed of a large number of electron beams (Poquérusse et al. 1996).

© Astronomical Society of the Pacific • Provided by the NASA Astrophysics Data System

1998ASPC..155..182K

from electron beams that travel from the low to the high corona and in the interplanetary space, yielding a burst which drifts from high to low frequencies (type III burst; Figure 3). The figure shows that a single type III burst at low frequencies is actually due to multiple beams injected at lower altitudes. During flares the beam signatures at short dm and cm-waves generally drift from low to high frequencies [often termed reverse slope (RS) bursts], indicating beams that propagate downward from the acceleration region in a plasma where $n_e \simeq 6 \cdot 10^9$ cm^{-3} (cf. Benz 1997, and references therein). Through these fast-drift bursts electron beams are tracers of the magnetic field topology, the thermal electron density, and of the sites and timing of elementary energy release processes in the corona.

3.2. Electron Beams Associated with Jets of Material in the Low Corona

The production of electron beams in association with jets of material in the low atmosphere has long been known from Hα and radio observations (Chiuderi-Drago et al. 1986, and references therein). Both Hα surges and type III bursts occur during the impulsive flare phase, but also in the absence of flares.

Chiuderi-Drago et al. (1986) showed by a systematic study of joint Hα and metre wave imaging observations that type III bursts occur together with surges in the same active region. The type III burst groups are not observed at the launch of the material jet, but most often around the time when its line-of-sight velocity is greatest. The authors argue that the electron beams are accelerated by a shock wave driven by the jet. Alternatively, Carbone et al. (1987) propose a model where internal instabilities of the expelled material, that propagates near a magnetic neutral line or with a sheared velocity field, decelerate the jet and produce the electric fields required for the electron acceleration.

More recently electron beams were found in conjunction with the expulsion of plasma visualised as soft X-ray jets (Aurass et al. 1994, Kundu et al. 1995, Raulin et al. 1996, van Driel-Gesztelyi et al. 1998). The association does not appear to be systematic, since among 16 X-ray jets listed by Shimojo et al. (1996) that occurred while the *Nançay Radioheliograph (NRH)* observed the Sun (five frequencies in the range 150 to 450 MHz; Kerdraon & Delouis 1997) only three had type III burst emission associated in space and time, while seven had no accompanying radio signatures (*NRH* quicklook data). The others were associated with long-lived noise storms with no conspicuous change at the time of the jets. Remarkably, two of the three jets associated with type III bursts occurred within three hours in the same active region. It is likely that here, as in the case of jets of cool material (Axisa et al. 1973), where the type III associated Hα events are situated at the border of the active region or near the line of photospheric magnetic field reversal, the global magnetic field structure in and around the active region plays a key role in determining whether a jet is associated with radio visible electron beams in the overlying corona or not. In the following, a few cases are discussed where type III bursts and X-ray jets are well associated, in an attempt to get some insight in the physical relationship between the two phenomena. Given that only a few single case studies exist so far, the conclusions are necessarily tentative.

© Astronomical Society of the Pacific • Provided by the NASA Astrophysics Data System

1998ASPC..155..182K

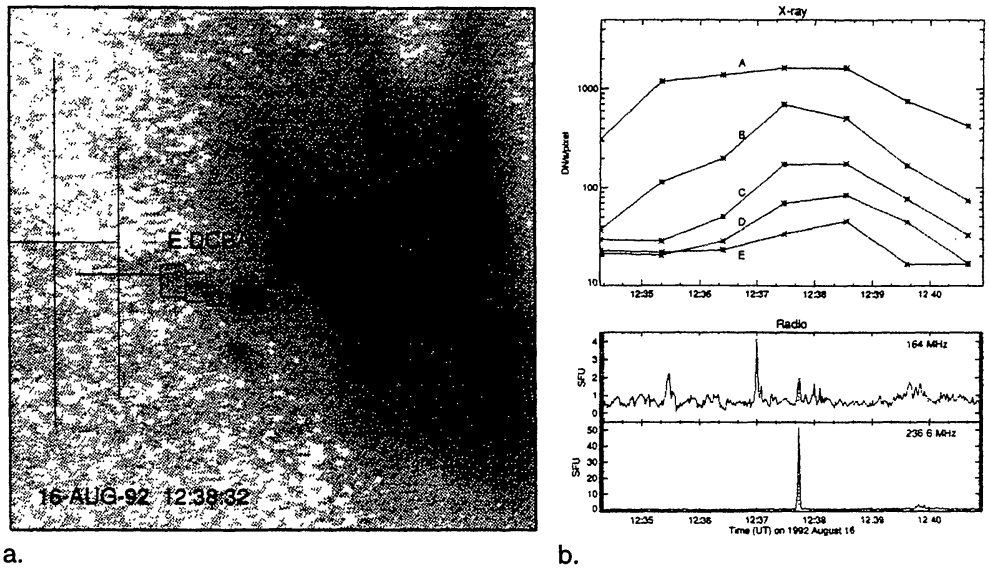

a. b.

Figure 4. Electron beams associated with a soft X-ray jet (Kundu et al. 1995). **a**: *Yohkoh-SXT* map (dark shading represents bright features) of the border of the parent active region in the north-eastern quadrant of the Sun, the location of a bright point (rectangle "A") and a jet ("B" - "E"). Radio sources (*Nançay Radioheliograph*, crosses give half widths measured with two orthogonal arrays) at 236.6 and 164 MHz (from right to left). **b**: Time histories of the brightness in the boxes A to E of the X-ray image (top) and of the radio flux densities (bottom).

The jet studied by Kundu et al. (1995, Figure 4) starts in the vicinity of an X-ray bright point (square "A" in Figure 4) in the outskirts of an active region. The plasma expands along the trajectory traced by the rectangles "B" to "E". The radio sources (crosses) lie along the extrapolated jet trajectory, in the order of decreasing frequency, i.e. decreasing thermal electron density. The electron densities inferred from the radio and X-ray data are consistent. Since the type III burst is isolated, its timing with respect to the jet evolution can be determined. It is evident that the burst occurs *after* the jet was launched: comparison of the X-ray brightening at the highest point where the jet can still be distinguished (E in Figure 4) with the radio time history (Figure 4.b) shows that the type III burst occurs at about the time when the ejected plasma reaches the projected position of the high-frequency radio source. This would be consistent with acceleration near the front of the jet. But in at least one other case (Raulin et al. 1996, their Figure 2.a) the electron beams propagate through the already existing jet material and can therefore not have been accelerated at its front. The electrons rather seem to be accelerated near the base of the jet, but minutes after the plasma has been ejected. This is consistent with all observations of type III burst associated jets, as shown by the compilation of published work in Table 1.

A possible site for the acceleration of the plasma jet and of the electron beams is the region where a complex magnetic polarity in the photosphere re-

© Astronomical Society of the Pacific • Provided by the NASA Astrophysics Data System

1998ASPC..155..182K

Table 1. Type III bursts associated with X-ray jets.

Authors	Flare	Speed of the jet [km s^{-1}]	Type III	Delay III -jet [min][a]	Geometry
Aurass et al. 1994	no	320	single	1	jet points towards III
Kundu et al. 1995	(no)	300-100[c]	single	>3	jet points towards III
Raulin et al. 1996	Hα, X [b]	250	group	4	?
	X	800	single	6	III travels through jet
van Driel-Gesztelyi	Hα, X	≥700	group	>4 ?	jet points towards III
et al. 1998	no	≥700	V Dm [d]	no obs.	no obs.

[a]using the extrapolated onset time of the jet
[b]GOES 1-8 Å (*Solar Geophysical Data - SGD*)
[c]deceleration observed
[d]short continuum at decametric waves (*SGD*)

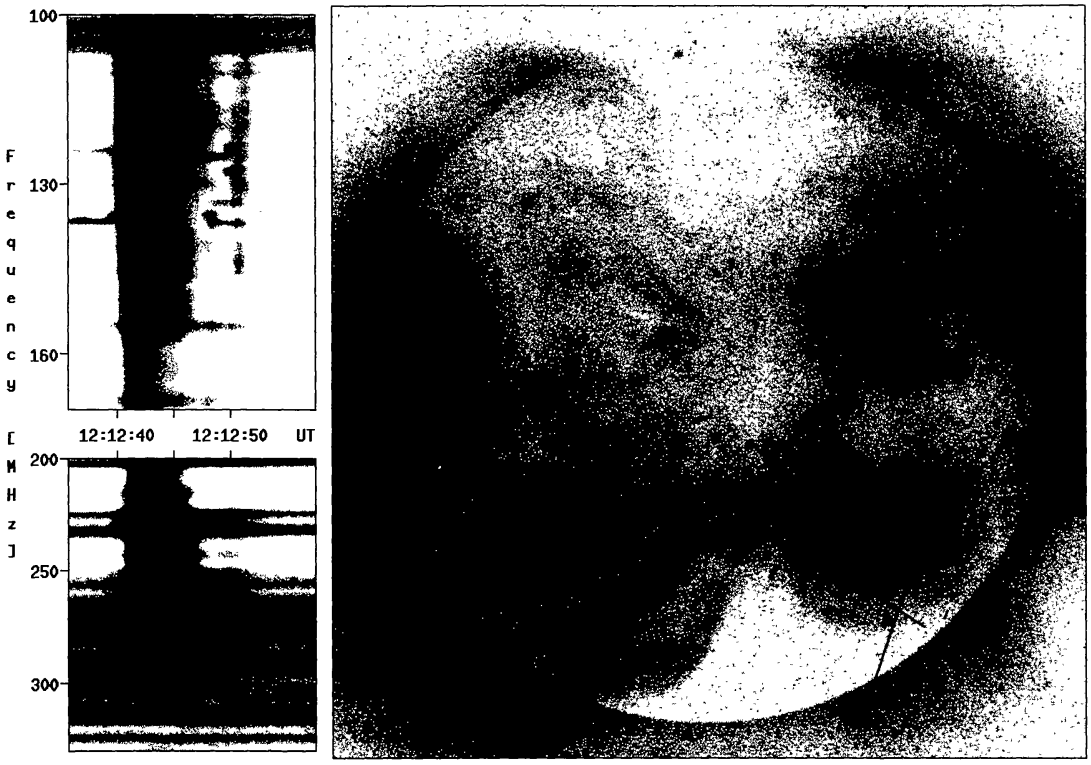

Figure 5. **a**: Spectrum of radio emission from electron beams injected in close succession into open (type III burst) and closed (type U) coronal structures (*Tremsdorf Radio Spectrograph*; dark shading denotes bright emission). **b**: Sources at 237 MHz (*Nançay Radioheliograph*) superposed on the *Yohkoh-SXT* map at 12:15 UT. Filled triangle: centroid of the type III burst. Crosses: centroid and half widths of the rising (solid) and descending (dashed) branch of the U burst. A soft X-ray jet is seen as an elongated brightening east of the parent active region (after Aurass et al. 1994).

© Astronomical Society of the Pacific • Provided by the NASA Astrophysics Data System

1998ASPC..155..182K

veals interaction of emerging with ambient magnetic field structures. Intrusions of magnetic field with opposite polarity are generally observed at the base of surges and of X-ray jets (e.g. Chiuderi-Drago et al. 1986, Canfield et al. 1996, Shibata 1997 and references therein). The event of Figure 5 (Aurass et al. 1994) confirms the launch of jets at the interface of magnetic structures with different connectivity: the spectrum at frequencies above 200 MHz (Figure 5.a) shows an initial type III burst extending to very low frequencies, i.e. electron beams that travel upward and probably to interplanetary space. Immediately afterwards a different spectral signature appears, consisting of a burst with initial type III-like frequency drift that turns over and eventually drifts towards higher frequencies again (since the spectrum has the shape of an inverted letter U, the feature is called a type U burst). The radio sources of the type U burst at 237 MHz (1.27 m; crosses in Figure 5.b) reveal electron beams propagating from south-east to north-west along the outer plasma loops of the underlying active region. The type III source due to electron beams travelling in open field structures (filled triangle in Figure 5.b) is slightly, but significantly displaced to the edge of the active region structures, as expected for an open flux tube. The electron beams must have been injected into a bundle of neighbouring field lines in the low corona, which separate at greater heights such as to produce the two distinct radio bursts. At the footpoints of these structures a jet appears as an elongated bright feature east of the parent active region in the *Yohkoh-SXT* image. The close temporal and spatial association between the jet and the two different radio bursts suggests strongly that the plasma jet and an ensemble of electron beams have been produced at the interface of regions of different magnetic connectivity.

The available observations of hot and cool jets associated with electron beams allow us to discard several possible interpretations of the physical relationship, provided a unique mechanism for this relationship exists: the electron beams cannot be accelerated at the interface between the jet and the corona into which it is propelled, e.g. by a shock wave, since electron beams have been observed in at least one event to travel through an already existing jet. The relative timing is also inconsistent with the idea that the electron beams are accelerated at the time when the jet is launched. Two possibilities seem to be consistent with all observations published so far: prolonged energy release at the base of the jet, i.e. through magnetic reconnection between emerging flux and preexisting structures, and internal instabilities of the jet. Both models require that the electron acceleration occur at the interface of different magnetic structures. Carbone et al.'s (1987) model based on internal instabilities of the jet considers the electron beam as a secondary phenomenon. It predicts a close link between the deceleration of the jet and particle acceleration. Kundu et al. (1995; cf. Table 1) infer that the speed of the plasma has started to decrease by the time the type III burst appears. Systematic observations with higher cadence and Doppler shift measurements in the EUV and X-ray range (cf. Shibata 1997) will be needed to complete the analysis.

3.3. Electron Acceleration in the Middle and High Corona

Electron beams which become first visible at coronal altitudes above roughly 0.5 $R_\odot$ are a frequent counterpart of complex active regions with noise storm

© Astronomical Society of the Pacific • Provided by the NASA Astrophysics Data System

1998ASPC..155..182K

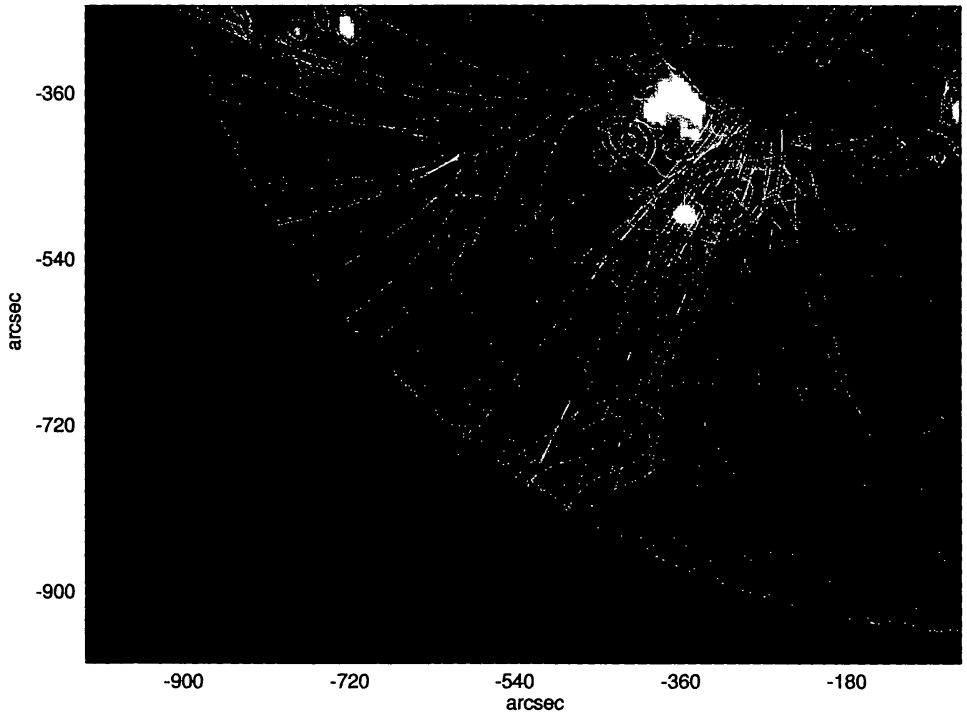

Figure 6. Radio sources in the corona (contour plots of equal brightness, *VLA*) superposed upon a Kitt Peak magnetogram and field lines from its current-free extrapolation (Krucker et al. 1995a). The southernmost radio source refers to metric spikes at 333 MHz (91 cm), revealing electron acceleration sites in the middle corona. The three radio sources above the active region are due to thermal emission at 1.4 GHz (21 cm).

emission at metre wavelengths. Outward travelling beams are revealed by type III bursts with starting frequency below about 100 MHz, i.e. much lower than those discussed in the previous section. Electron beams with energies up to ~10 keV are detected by satellites near the Earth (Lin 1985, 1997, Kayser et al. 1987, Dulk 1990). They are the most frequent transient electron populations of solar origin at 1 AU. Upon travelling from the acceleration site to the detector, the electrons lose energy through Coulomb collisions with ambient electrons. This will deplete the low-energy part of the particle spectrum. But since a power-law spectrum is observed to extend most often down to 2 keV without any signature of Coulomb losses, the acceleration site must be in a tenuous plasma, at heights greater than 0.2 to 0.5 $R_\odot$ above the photosphere (Lin 1985, 1997), depending on the adopted coronal density model. Since the electron populations under discussion are in general produced without major energy release in the low atmosphere (e.g. a flare), there is no large-scale perturbation like a shock wave running through the corona. The acceleration must occur in more long-lived structures. The current sheet of a coronal streamer has been suggested on theoretical grounds by Gubchenko & Zaitsev (1983) and Cliver & Kahler

© Astronomical Society of the Pacific • Provided by the NASA Astrophysics Data System

1998ASPC..155..182K

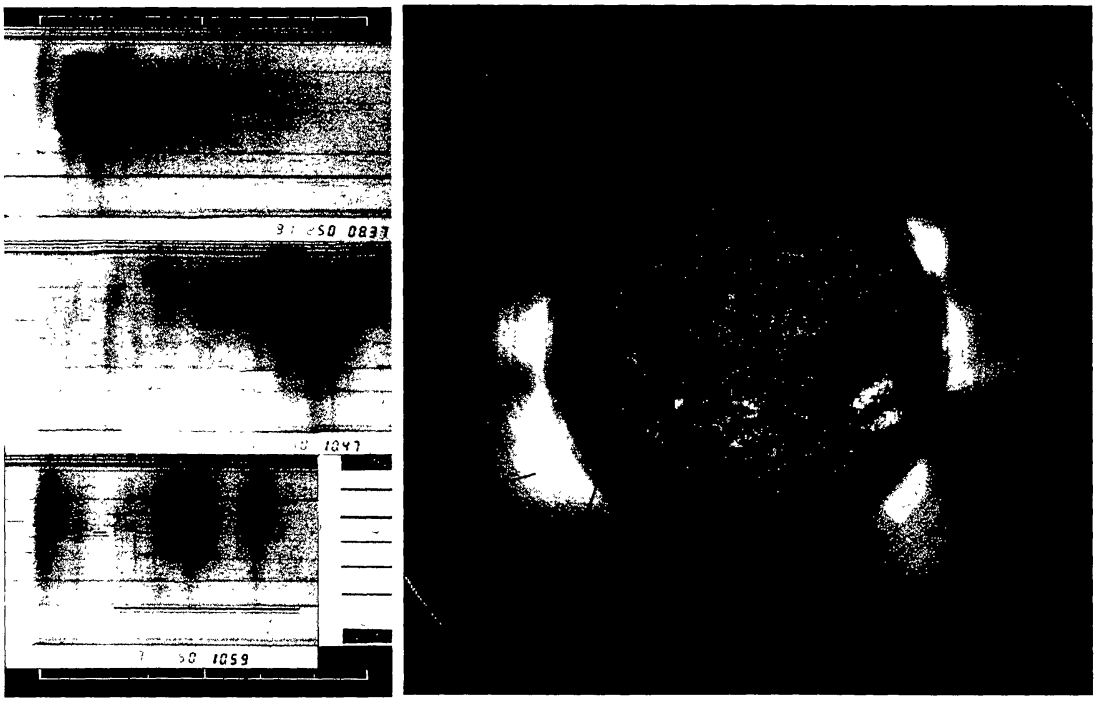

a. b.

Figure 7. **a**: Spectra (100-170 MHz) of three groups of fast-drift (III, RS) bursts. The white horizontal lines above and below the plots indicate 1 min duration. **b**: Sources (crosses) at 164 MHz during the two brightest RS bursts of the first event, on top of a Mauna Loa image of the white-light corona (taken 15 hours before the bursts) and a Meudon Hα spectroheliogram (after Klein et al. 1997).

(1991). Sensitive radio observations enable us now to confront these ideas with observations.

Krucker et al. (1995a; cf. also Krucker et al. 1997) analyzed *VLA* observations of nonthermal and thermal electron populations at 333 MHz (91 cm) and 1.4 GHz (21 cm). No Hα flare is reported at the time of the radio emission. The low-frequency emission has the narrow bandwidth and rapid variation known from decimetric spikes during impulsive flares. The source (Figure 6: southernmost radio source plotted as iso-intensity contours) seems to be located at a height of 0.65 $R_\odot$ above the photosphere, in a bundle of open field lines inferred from the current-free extrapolation of the photospheric magnetic field. At lower altitude several thermal sources (λ=21 cm) are observed. The plasma at the footpoints of the field lines through the spike source brightens about 40 s after the spikes, while outward travelling electron beams are seen at longer wavelengths, i.e. greater altitude than the spike source. These observations suggest that energy is released, and electrons are accelerated, near the spike source in the middle corona. Energy transport to the low corona along magnetic field lines heats the plasma such as to enhance the brightness of the 21 cm source.

It is not clear to which kind of magnetic structure belong the apparently open field lines that Krucker et al. infer at the acceleration site, and how energy

© Astronomical Society of the Pacific • Provided by the NASA Astrophysics Data System

1998ASPC..155..182K

might be released there. Klein et al. (1997) observed reverse slope (RS) bursts at metre wavelengths. The drift from low to high frequencies (Figure 7.a) reveals electron beams travelling downward through the corona. When mapped near its high-frequency limit (164 MHz/1.83 m, crosses in Figure 7.b), each RS burst corresponds to the simultaneous brightening at two sites separated by 0.7 to 0.9 $R_\odot$ which project to either side of a coronal streamer. Since the individual RS bursts must have been accelerated in a rather small volume in order to display such a well-organized spectral signature, the authors conclude that the beams were injected on nearly parallel field lines about 1 $R_\odot$ above the photosphere, and that the field lines separate at lower altitude. The configuration suggests that the electrons were accelerated in the current sheet of a coronal streamer. The RS bursts occur within groups of ordinary type III bursts due to electron beams accelerated upward in the low corona (e.g. Figure 7.a, centre). The source of the III bursts is near the northernmost source of the RS bursts in Figure 7.b. The beams must have been accelerated in an active region at or behind the limb. The three burst groups occur while the whole large-scale coronal structure is gradually evolving in response to the emergence of magnetic flux in at least two active regions underneath the span of the streamer, indicated by small plages in the south-eastern quadrant of the Sun in Figure 7.b. This configuration stores energy that is released at widely different places, including sites in the high corona where electron beams detected at 1 AU might be accelerated.

4. Quasi-steady Electron Acceleration in the Middle Corona

Noise storms are the oldest known radio signature of the Sun. They are associated with active regions, especially with large sunspot groups, sometimes with flares or coronal mass ejections, but occur most often without conspicuous activity in the underlying atmosphere and last much longer than flares, up to several days. The spectrum is composed of broadband continuum emission from decimetric to metric wavelengths ($\Delta\nu/\nu \sim 1$) and superposed short-lived (≤ 1 s) narrow-band ($\Delta\nu/\nu \leq 0.03$) bursts. Bursts and continuum have brightness temperatures far above the coronal electron temperature and are in general nearly 100 % circularly polarized. At decametric wavelengths storms of type III bursts, i.e. electron beams travelling through the high corona towards interplanetary space, often accompany noise storms in the underlying corona.

The high circular polarization of the noise storm continuum (in the ordinary mode of magnetoionic theory; Elgarøy 1977) implies collective plasma emission, yielding electromagnetic waves near the electron plasma frequency. The radiating electrons have no beam distribution, but are thought to be trapped in large-scale magnetic field structures. A gross estimate of the energy carried by these electrons can be obtained as follows: if broadband fluctuations of the continuum (Gnezdilov & Fomichev 1987, Raulin & Klein 1994) are due to the injection of freshly accelerated electrons into the large-scale loops, the observed bandwidth of the fluctuations (~ 300 MHz) implies that the electrons must have energies of at least 10 keV in order to survive Coulomb collisions while travelling between the corresponding plasma levels (Raulin & Klein 1994). The lifetime of these electrons does not exceed a few tens of seconds. Hence electrons must be accelerated throughout the duration of the noise storm. The rate of energy

© Astronomical Society of the Pacific • Provided by the NASA Astrophysics Data System

1998ASPC..155..182K

release (ignoring ions for which there is no diagnostic available) is of the order of $10^{23} - 10^{25}$erg s^{-1} (cf. Klein 1994, and references therein). Considering a typical source dimension of 10^{10} cm, the energy flux required to maintain the nonthermal electron population is $10^3 - 10^5$erg cm^{-2} s^{-1}, i.e. smaller than coronal energy losses.

Noise storms are therefore not a challenge to energy transport and storage, but an illustration of nonthermal processes involving small rates of energy release. While their common occurrence and long duration demonstrate that noise storms are related with the general evolution of coronal structures, the association with complex and rapidly evolving active regions (see below) suggests that coronal currents play an important part in their development. The study of noise storms can hence further our understanding of both the evolution of the corona and of explosive energy release processes, which can be studied in a less perturbed environment in noise storms than during flares. In the following some imaging observations are presented. The many earlier works which provided to a large extent the basis for contemporary models are discussed in Elgarøy's monograph (1977) and in the review by Kai et al. (1985).

4.1. Noise Storms and Global Coronal Evolution

Observations by *Skylab* and the *Culgoora Radioheliograph* (Stewart et al. 1986) showed that noise storms arise in and evolve with large-scale coronal loop systems. They are also identified in soft X-ray images and in potential extrapolations of the photospheric magnetic field (Ambrož 1983, Krucker et al. 1995b). Bogod et al. (1995) observed noise storms with the *VLA* and the coronal plasma structures with *Yohkoh-SXT* and also considered the evolution of the sunspot configuration in the underlying active region. They compared the day-to-day evolution of noise storms in a large complex active region (Figure 8, AR 7496/ 7500 at the north-eastern limb on May 6) and a smaller, but rapidely evolving region (AR 7499, emerging near disk centre). On May 8 the noise storm above the large active region has disappeared while the bulk of the bright large-scale X-ray loops persisted. A new noise storm has developed above the much smaller, but more rapidly evolving AR 7499. Comparison with the multi-frequency observations of the *Nançay Radioheliograph* (frequencies at which the noise storm is observed are noted in the insets of Figure 8) shows that rather than a sudden disappearance and appearance of the noise storms, one sees a gradual frequency shift: the "old" noise storm above the north-eastern active region shifts to lower frequencies and thereby becomes invisible to the *VLA* on May 8, and one day later to the *NRH*. Some of the bright loops seen by *Yohkoh* also change shape or disappear. The new noise storm above AR 7499 is not visible at the lowest *NRH* frequency on May 8, but appears there one day later. These observations suggest that the noise storm emission occurs in magnetic structures which gradually, on a day-to-day basis, become more dilute either because of the evolution of the active region plasma or since the energy release region and the regions accessible to the accelerated electrons shift to greater heights. Stewart et al. (1986) propose a scenario where magnetic flux emerges within a new active region amongst pre-existing magnetic structures. As the new flux penetrates into the overlying structures, reconnection creates links with pre-existing active regions. In this way new magnetic loops form at successively greater heights as the footpoints

© Astronomical Society of the Pacific • Provided by the NASA Astrophysics Data System

1998ASPC..155..182K

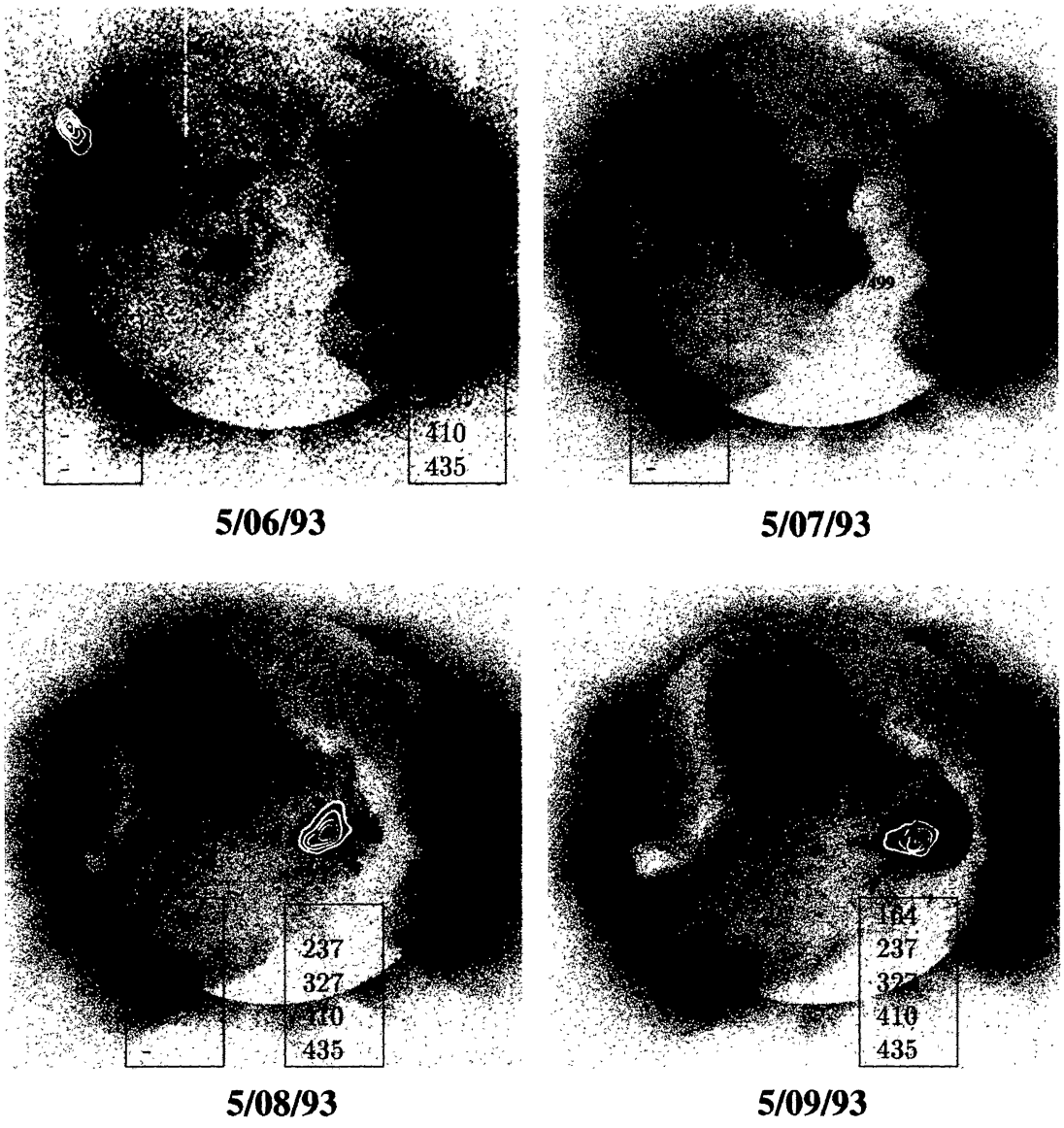

Figure 8. Contours of equal brightness of noise storm emission observed with the *VLA* at 327 MHz (91 cm), superposed upon *Yohkoh* soft X-ray images of the corona on four consecutive days (Bogod et al. 1995). The inserted frames give the frequencies at which the noise storms are seen by the *Nançay Radioheliograph* from about 9 to 15 UT each day. No *VLA* observations are available on May 7.

© Astronomical Society of the Pacific • Provided by the NASA Astrophysics Data System

1998ASPC..155..182K

of the newly emerging active region spread. The typical speed of upward expansion that Stewart et al. (1986) infer from their XUV and radio observations, 1 - 2 km s^{-1}, is consistent with the typical speed at which emerging sunspots separate. Krucker et al.'s (1995b) gradual shift, at a few km/s, of the source in the course of a noise storm is consistent with the loop expansion expected in response to magnetic flux emergence. The gradual extension of the noise storm emission to lower frequencies (Figure 8) is predicted by this scenario.

When noise storms evolve through the reconnection of magnetic fields in the middle corona, implying small amounts of magnetic energy, no counterpart in Hα or X-ray emission from the underlying active region should be expected, and none is observed. But structural changes in the corona are seen at the *onset* of noise storms: Kerdraon et al. (1983) showed that the onset or enhancement of noise storms are systematically associated with a restructuring of the corona revealed by narrow features in white-light observations, much smaller than loop-shaped coronal mass ejections. Reconfigurations of active region structures prior to or at the onset of noise storms, occurring on time scales of a few minutes to tens of minutes, are seen in microwaves and soft X-rays (Raulin et al. 1991, Raulin & Klein 1994). These phenomena may include electron acceleration up to $\sim$ 10 keV (Crosby et al. 1996), reminiscent of weak flares. The X-ray response shows that the onset of noise storms is related with energy conversion in the active region. On time scales of some minutes to a few tens of minutes the radio signature shifts to lower frequencies, i.e. into more dilute coronal structures. Typical expansion speeds in this phase are several tens of km s^{-1} (Raulin & Klein 1994). In a few cases (Lantos et al. 1981, Švestka et al. 1982) the noise storm emission coevolves with the soft X-rays, but most often the radio emission continues without X-ray counterpart (Raulin & Klein 1994, Crosby et al. 1996). This again suggests that the energy release proceeds to greater altitudes, where the dissipated power is not sufficient to create a conspicuous response in the thermal active region plasma.

The scenario suggested by these observations contradicts models where the noise-storm emitting electrons are accelerated in the current sheet of a coronal streamer (e.g. Gubchenko & Zaitsev 1983). It is noted that during the bursts of Figure 7, where evidence for acceleration in a streamer is shown, no noise storm was observed at decimetric and metric wavelengths. On the other hand these current sheets are promising sites for the acceleration of electron beams detected near 1 AU, and these beams are associated with active regions having noise storms (Kayser et al. 1987). This may be another hint to acceleration in different parts of a large-scale coronal structure, as already discussed with respect to Figure 7.

4.2. Cessation of Noise Storm Emission

A trivial consequence of the picture that noise storms occur in large-scale coronal loops is that the radio emission ceases when the loop disappears, as actually observed by Stewart et al. (1986, cf. e.g. their Figure 6). In a more energetic event Lantos et al. (1981; cf. also Hildner et al. 1986) observed that a noise storm was displaced in the course of a coronal mass ejection and faded together with the soft X-ray event in the underlying active region. Since a mass ejection implies the reconfiguration on large spatial scales, the observation fits with the

© Astronomical Society of the Pacific • Provided by the NASA Astrophysics Data System

1998ASPC..155..182K

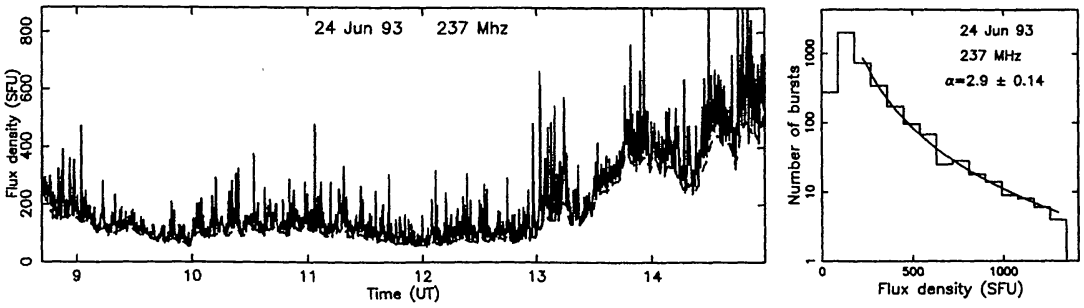

Figure 9. **a**: Flux density of a noise storm. The dashed line denotes the contribution of the broadband continuum emission. **b**: Frequency distribution of the flux density of the bursts (histogram) together with a power-law fit with index 2.9 (solid curve; Mercier & Trottet 1997).

idea that large-scale closed magnetic structures are a prerequisite for a noise storm. A different mechanism might cause the temporary suppression of noise storm emission (Böhme & Krüger 1982, Aurass et al. 1993, Zaitsev et al. 1994). The depression of noise storm emission during microwave bursts, as well as the gradual spread of the depression to successively lower frequencies observed in several cases, are suggestive of extinction by rising material, e.g. due to chromospheric evaporation, or by a travelling MHD perturbation launched in the low atmosphere (Aurass 1997 and references therein).

4.3. Small-scale Structure of Noise Storm Sources

Upon closer scrutiny with imaging instruments, the global configuration in which noise storms evolve has intrinsic structure. This shows up through discrete positional changes of noise storm continuum sources, which appear to be random when observed during several hours at a single frequency (Krucker et al. 1995b), but may occur in a coordinated manner at different frequencies (Malik & Mercier 1996). A noise storm continuum source hence consists of several substructures with individual lifetimes of the order of an hour. This is roughly consistent with the lifetime of large-scale plasma loops (e.g. Bray et al. 1991). When one such substructure is extinguished, or a new one illuminated, the centroid position of the noise storm continuum suddenly shifts by a fraction of the global source dimension at a given frequency. This shows that while large-scale active region evolution sets the stage for the noise storm emission, the intrinsic scales are smaller, as expected from the finer structures seen in X-ray images.

Given the lifetime of the radiating electrons, the acceleration process in noise storms must be repetitive on timescales of a few to a few tens of seconds. Figure 9.a displays the time evolution of noise storm emission during several hours. The bursts superposed on the slowly evolving continuum (dashed line) are readily visible. Their short duration, narrow bandwidth and the fact that their positions scatter over the extent of the continuum source (Malik & Mercier 1994 Figure 3, Willson et al. 1997 Figure 14) suggest that they might reveal sites of elementary energy release within the large-scale structures that host

© Astronomical Society of the Pacific • Provided by the NASA Astrophysics Data System

1998ASPC..155..182K

the continuum emission (cf. also Benz & Wentzel 1981, Spicer et al. 1981). Mercier & Trottet (1997) gave further evidence for this by analysing the number of bursts as a function of their peak flux density. The distribution (Figure 9.b) follows a power law like other tracers of energy release in the corona (e.g. hard X-ray bursts [Crosby et al. 1993], transient brightenings of active regions in soft X-rays [Shimizu 1995]), but with a steeper slope. The meaning of this slope in terms of elementary energy release processes is still open, because the emission involves non linear processes so that the flux density is not related in a simple way with the energy carried by the radiating electrons. This problem deserves further study, since noise storm continua and the associated bursts illustrate the relationship of processes of solar activity acting on very different spatial and temporal scales (cf. Bastian & Vlahos 1997, and references therein).

5. Summary and Conclusions

Radio emission at decimetric and longer wavelengths shows suprathermal electrons to be a ubiquitous population in the active region corona. Not all radio bursts discussed here are unambiguously associated with primary energy release processes: the relationship between material jets and electron beams is consistent with the idea that both result from a primary energy release process such as reconnection, but also with the opposite view that the electron beams are a secondary phenomenon produced by internal instabilities of the jet.

However, the noise storms and downward propagating electron beams do result from acceleration in the middle and high corona, i.e. in the range $\sim 0.1 - 1$ $R_\odot$ or more above the photosphere. The acceleration shares characteristics with energy release observed during flares:

- Electron beams are a basic population irrespective of whether the event is part of a flare or not. This suggests that energy is released in discrete steps ("fragmented" energy release, cf. Bastian & Vlahos 1997). Narrow-band bursts on still shorter timescales may be further evidence of fragmentation. In non-flaring active regions these small-scale phenomena may occur during several days.

- Particle acceleration in the middle and high corona takes place in configurations which evolve in response to changing conditions in the underlying atmosphere. These can often be ascribed to the emergence of magnetic flux, even when the energy release occurs far from the photosphere.

Energy release in the middle and high corona is difficult to probe during flares, since the bright (X-ray) emission from the denser plasma at lower altitudes dominates. When this emission is occulted by the photosphere, low-energy electrons accelerated in the middle corona become visible (Kane et al. 1992). These electron populations have no conspicuous response in the thermal plasma emissions, presumably both because they carry little energy and because the convergence of the magnetic field and Coulomb collisions prevent beams from penetrating in the low corona. A close relationship seems to exist between coronal acceleration and particle populations injected into interplanetary space. The energy spectra of low-energy impulsive electron events (Lin 1985, 1997) and the

© Astronomical Society of the Pacific • Provided by the NASA Astrophysics Data System

1998ASPC..155..182K

ionization states during major solar energetic particle events (Ruffolo 1997) imply that the particles have traversed a small amount of coronal material, hence must have been accelerated high above the photosphere. Particle acceleration sites probed by the radio emission in non-flaring active regions might therefore be relevant to understanding the connection between particles interacting in the low atmosphere and those detected *in situ*.

While the elementary acceleration processes are short and occur in small volumes, their repetitive operation and distribution within large-scale coronal structures make the global process extended in space and time. How, where and when the evolution of the large-scale structures creates conditions for small-scale energy release is not clear, but the understanding of this coupling is crucial for any form of energy release in the corona (cf. Miller et al. 1997), and will allow us to decide to which extent basic manifestations of solar activity are physically similar or not. There is a chance that in the case of low-energy events outside flares the environment in which energy is released is less perturbed, which would make the identification of physically significant associations easier. This is a major task for joint observations with *SoHO*.

Acknowledgments. The author thanks the organizers of the ASPE Conference for a stimulating meeting and for the invitation to give this review. He is indebted to the colleagues who made their illustrations available, and to D. Maia and F. Daulny for help with the figures. The generous supply of daily images from the *Yohkoh* and *SoHO* missions is acknowledged. The bibliographical research of the present paper has largely benefitted from the *NASA Astrophysics Data System Abstract Service.*

References

Ambrož P. 1983, Pub. Debrecen Heliophys. Obs. 5, 145

Aurass H. 1997, in Coronal Physics from Radio and Space Observations, G. Trottet, Lecture Notes in Physics 483, Berlin: Springer, 135

Aurass H., Hofmann A., Magun A., Soru-Escaut I., & Zlobec P. 1993, Solar Phys. 145, 151

Aurass H., Klein K. -L., & Martens P. C. H. 1994, Solar Phys. 155, 203

Axisa F., Martres M. J., Pick M., & Soru-Escaut I. 1973, Solar Phys. 29, 163

Bastian T. S., & Vlahos L. 1997, in Coronal Physics from Radio and Space Observations, G. Trottet, Lecture Notes in Physics 483, Berlin: Springer, 68

Benz A. O., & Wentzel D. G. 1981, A&A 94, 100

Benz A. O. 1993, Plasma Astrophysics, Dordrecht: Kluwer

Benz A. O. 1994, in Coronal Magnetic Energy Releases, A. O. Benz, A. Krüger, Lecture Notes in Physics 444, Berlin: Springer, 1

Benz A. O. 1997, in Solar and Heliospheric Plasma Physics, G. M. Simnett, C. E. Alissandrakis, L. Vlahos, Lecture Notes in Physics 489, Berlin: Springer, 201

Böhme A., & Krüger A. 1982, Solar Phys. 76, 63

Bogod V. M., & Garimov V., Gelfreikh G. B. et al. 1995, Solar Phys. 160, 133

© Astronomical Society of the Pacific • Provided by the NASA Astrophysics Data System

1998ASPC..155..182K

Bray R. J., Cram L. E., Durrant C. J., & Loughhead R. E. 1991, Plasma Loops in the Solar Corona, Cambridge: Cambridge University Press, ch. 3. 4.

Canfield R. C., & Reardon K. P., Leka K. D. et al. 1996, ApJ 464, 1016

Carbone V., Einaudi G., & Veltri P. 1987, Solar Phys. 111, 31

Chiuderi-Drago F., Mein N., & Pick M. 1986, Solar Phys. 103, 235

Cliver E., & Kahler S. 1991, ApJ 366, L91

Crosby N., Aschwanden M. J., & Dennis B. R. 1993, Solar Phys. 143, 275

Crosby N., Vilmer N., Lund N., Klein K. -L., & Sunyaev R. 1996, Solar Phys. 167, 333

Dulk G. A. 1990, Solar Phys. 130, 139

Elgarøy Ø. 1977, Solar Noise Storms, Oxford: Pergamon Press

Gnezdilov A. A., & Fomichev V. V. 1987, Soviet Astron. Lett. 13, 297

Gubchenko V. M., & Zaitsev V. V. 1983, Solar Phys. 89, 391

Hildner E., & Bassi J., Bougeret J. -L. et al. 1986, in Energetic Phenomena on the Sun, M. R. Kundu, & B. E. Woodgate, NASA CP-2439, 6-1

Hudson H. S. 1991, Solar Phys. 133, 357

Kai K., Melrose D. B., & Suzuki S. 1985, in Solar Radiophysics, D. J. McLean, & N. R. Labrum, Cambridge: Cambridge University Press, 415

Kane S. R., & McTiernan J. M., Loran J. et al. 1992, ApJ 390, 687

Kane S. R., & Hurley K., McTiernan J. M. et al. 1995, ApJ 446, L47

Kayser S., Bougeret J. -L., Fainberg J., & Stone R. G. 1987, Solar Phys. 109, 107

Kerdraon A., & Delouis J. -M. 1997, in Coronal Physics from Radio and Space Observations, G. Trottet, Lecture Notes in Physics 483,Berlin: Springer, 192

Kerdraon A., & Pick M., Trottet G. et al. 1983, ApJ 265, L19

Klein K. -L. 1994, in Coronal Magnetic Energy Releases, A. O. Benz, & A. Krüger, Lecture Notes in Physics 444, Berlin: Springer, 55

Klein K. -L., Aurass H., Soru-Escaut I., & Kálmán B. 1997, A&A 320, 612 (Erratum with correctly printed figures in A&A 322, 1027)

Krucker S., Aschwanden M. J., Bastian T. S., & Benz A. O., 1995a, A&A 302, 551

Krucker S., Benz A. O., Aschwanden M. J., & Bastian T. S. 1995b, Solar Phys. 160, 151

Krucker S., Benz A. O., & Aschwanden M. J. 1997, A&A 317, 569

Kundu M. R., Raulin J. P., Pick M., & Strong K. T. 1995, ApJ 444, 922

Lantos P., & Alissandrakis C. E. 1996, Solar Phys. 165, 61

Lantos P., Kerdraon A., Rapley G. G., & Bentley R. D. 1981, A&A 101, 33

Lantos P., Alissandrakis C. E., Gergely T., & Kundu M. R. 1987, Solar Phys. 112, 325

Lin R. P., 1985, Solar Phys. 100, 537

Lin R. P., 1997, in Coronal Physics from Radio and Space Observations, G. Trottet, Lecture Notes in Physics 483,Berlin: Springer, 93

© Astronomical Society of the Pacific • Provided by the NASA Astrophysics Data System

1998ASPC..155..182K

Malik R. K., & Mercier C. 1996, Solar Phys. 165, 347

Melrose D. B. 1980, Spa. Sci. Rev. 26, 3

Mercier C., & Trottet G. 1997, ApJ 474, L65

Miller J. A., & Cargill P. J., Emslie A. G. et al. 1997, JGR 102, 14631

Poquérusse M., Hoang S., & Bougeret J. -L., Moncuquet M. 1996, in Solar Wind 8, D. Winterhalter e al., Woodbury: AIP Press, 62

Raulin J. P., & Klein K. -L. 1994, A&A 281, 536

Raulin J. P., & Willson R. F., Kerdraon A. et al. 1991, A&A 251, 298

Raulin J. P., Kundu M. R., Hudson H. S., Nitta N., & Raoult A. 1996, A&A 306, 299

Ruffolo D. 1997, ApJ 481, L119

Sheridan K. V., & McLean D. J. 1985, in Solar Radiophysics, D. J. McLean, N. R. Labrum, Cambridge: Cambridge University Press, 442

Shibata K. 1997, in The Corona and SolarWind Near Minimum Activity, ESA SP-404, 103

Shimizu T. 1995, PASJ 47, 251

Shimojo M., & Hashimoto S., Shibata K. et al. 1996, PASJ 48, 123

Spicer D. S., Benz A. O., & Huba J. D. 1981, A&A 105, 221

Stewart R. T., Brueckner G. E., & Dere K. P. 1986, Solar Phys. 106, 107

Švestka Z., & Dennis B. R., Pick M. et al. 1982, Solar Phys. 80, 143

van Driel-Gesztelyi L., & Willson R. F., Kile J. N. et al. 1998, in 10th Cambridge Workshop Cool Stars, Stellar Systems and the Sun, in press

Vilmer N., Trottet G. 1997, in Coronal Physics from Radio and Space Observations, G. Trottet, Lecture Notes in Physics 483,Berlin: Springer, 28

Willson R. F., Kile J. N., & Rothberg B. 1997, Solar Phys. 170, 299

Zaitsev V. V., Aurass H. Krüger A., & Mann G. 1994, A&A 291, 990

© Astronomical Society of the Pacific • Provided by the NASA Astrophysics Data System